

Asymptotic model for shape resonance control of diatomics by intense non-resonant light: Universality in the single-channel approximation

Anne Crubellier,^{1,*} Rosario González-Férez,^{2,3,†} Christiane P. Koch,^{4,‡} and Eliane Luc-Koenig^{1,§}

¹*Laboratoire Aimé Cotton, CNRS, Université Paris-Sud 11,
ENS Cachan, Bâtiment 505, 91405 Orsay Cedex, France*

²*Instituto Carlos I de Física Teórica y Computacional and Departamento de Física Atómica,
Molecular y Nuclear, Universidad de Granada, 18071 Granada, Spain*

³*The Hamburg Center for Ultrafast Imaging, University of Hamburg,
Luruper Chaussee 149, 22761 Hamburg, Germany*

⁴*Theoretische Physik, Universität Kassel, Heinrich-Plett-Str. 40, 34132 Kassel, Germany*

(Dated: November 2, 2021)

Non-resonant light interacting with diatomics via the polarizability anisotropy couples different rotational states and may lead to strong hybridization of the motion. The modification of shape resonances and low-energy scattering states due to this interaction can be fully captured by an asymptotic model, based on the long-range properties of the scattering [Crubellier et al. [arXiv:1412.0569](#)]. Remarkably, the properties of the field-dressed shape resonances in this asymptotic multi-channel description are found to be approximately linear in the field intensity up to fairly large intensity. This suggests a perturbative single-channel approach to be sufficient to study the control of such resonances by the non-resonant field. The multi-channel results furthermore indicate the dependence on field intensity to present, at least approximately, universal characteristics. Here we combine the nodal line technique to solve the asymptotic Schrödinger equation with perturbation theory. Comparing our single channel results to those obtained with the full interaction potential, we find nodal lines depending only on the field-free scattering length of the diatom to yield an approximate but universal description of the field-dressed molecule, confirming universal behavior.

PACS numbers: 34.50.Cx,34.50.Rk

I. INTRODUCTION

Quantum collisions at low energy depend on the long-range properties of the interaction between the particles only and therefore exhibit universal behavior. Since, at long range, the dependence of the interaction on interparticle distance has a power-law form and it is often sufficient to account only for the highest order term of the interaction, low-energy collisions can be well described by simple models with very few free parameters. This is at the core of multi-channel quantum defect theory [1–8]. Universality becomes particularly transparent when introducing units which absorb all molecule-specific parameters [9]. The corresponding Schrödinger equation can be solved by the so-called nodal line technique [10–12]. It consists in accounting for all short-range physics by the choice of position of the nodes of the scattering wavefunction at intermediate interparticle distances. This formalism has been extended to shape resonances [13] and to the control of shape resonances by non-resonant light which couples the different partial ℓ -waves via the polarizability anisotropy [14]. In particular, we have previously shown that an intensity-dependent nodal line is sufficient to account for the effect of the coupling to the

non-resonant light at short-range. An asymptotic multi-channel model can thus predict the resonance structure, energy, width and hybridization as a function of non-resonant light intensity. This is important since non-resonant light control has been suggested to enhance photoassociation rates [15, 16], modify Feshbach resonances [17] and manipulate molecular levels [16, 18].

While a multi-channel treatment is essential to describe the strong hybridization of the rovibrational motion due to the coupling with the non-resonant light [15, 16], the position and width of the resonance are found to vary linearly with field intensity up to fairly large intensities [14]. When treating the interaction with the non-resonant light as a perturbation and truncating the perturbation expansion at the first order, resonance position and width are determined by the field-free wavefunctions. The field-free wavefunctions reside in a single partial wave (channel) and, within the asymptotic approximation, depend on only one parameter – the background scattering length. This indicates universality of the intensity dependence of resonance positions and widths in non-resonant light control. It furthermore suggests that a single-channel approach should be sufficient to study non-resonant light control at moderate intensities.

Here we combine the asymptotic model for shape resonance control with non-resonant light developed in a preceding paper [14] with perturbation theory to explore the universality of the resonance’s intensity dependence. This allows us to recast the multi-channel approach of Ref. [14] in a single channel approximation.

*Electronic address: anne.crubellier@u-psud.fr

†Electronic address: rogonzal@ugr.es

‡Electronic address: christiane.koch@uni-kassel.de

§Electronic address: eliane.luc@u-psud.fr

We compare the perturbative results to those obtained in Ref. [14] with a multi-channel description, by solving the Schrödinger equation for the diatom interacting with non-resonant light both with the full potential and the asymptotic approximation.

The paper is organized as follows: We briefly review the asymptotic model for a diatomic interacting with non-resonant light via the polarizability anisotropy introduced in Ref. [14], hereafter referred to as paper I, in Sec. II. We summarize the behavior of shape resonances in non-resonant light observed by solving the multi-channel Schrödinger equation and present an approximate general law for describing the intensity dependence when analyzing the resonances in reduced units of length and energy in Sec. III. We then show in Sec. IV how perturbation theory, either using energy-normalized continuum states (Sec. IV A) or a discretized continuum (Sec. IV B), is applied to determine the slopes of the intensity dependence of position and width of the field-dressed shape resonances at vanishing intensity. This allows us to explain the rule observed for the specific example of strontium dimers considered in paper I. Then, section Sec. V A describes systematic single-channel calculations that allow for predicting the position and width of shape resonances without a non-resonant field. These results are used in Sec. V B to deduce the slope of the energy shifts of a shape resonance in the limit of vanishing intensity for any angular momentum ℓ , in any diatomic system. We conclude in Sec. VI.

II. ASYMPTOTIC MODEL FOR A DIATOM IN A NON-RESONANT OPTICAL FIELD

In this section, we summarize the theoretical framework for studying the interaction of a diatom with non-resonant light. A detailed derivation of the asymptotic model is found in Ref. [14]. The Hamiltonian of an atom pair, with reduced mass μ , interacting with a non-resonant laser field of intensity I , linearly polarized along the space-fixed Z axis, is written in the molecule-fixed frame as

$$H = T_R + \frac{\mathbf{L}^2}{2\mu R^2} + V_g(R) - \frac{2\pi I}{c} (\Delta\alpha(R) \cos^2 \theta + \alpha_{\perp}(R)). \quad (1)$$

Here, R denotes interatomic separation and $V_g(R)$ the interaction potential in the electronic ground state. T_R and $\mathbf{L}^2/2\mu R^2$ are the vibrational and rotational kinetic energies. In the last term of Eq. (1), c is the speed of light and θ the polar angle between the molecular axis and the laser polarization. The molecular polarizability tensor is characterized by its perpendicular and parallel components with respect to the molecular axis $\alpha_{\perp}(R)$ and $\alpha_{\parallel}(R)$, and the polarizability anisotropy is $\Delta\alpha(R) = \alpha_{\parallel}(R) - \alpha_{\perp}(R)$. The non-resonant field introduces a mixing of different partial waves ℓ of the same parity (channels), whereas the magnetic quantum number m is conserved. The corresponding multi-channel Schrödinger equation can be

solved numerically as described in Ref. [16].

At sufficiently large distance, $R > R_{asym} = \sqrt{C_8/C_6}$, the potential reduces to the asymptotic van der Waals interaction $V_g(R) \approx -C_6/R^6$ (C_n are the coefficients of the multipolar expansion). For $R > R_d = (4\alpha_1\alpha_2)^{1/6}$, where α_1, α_2 denote the polarizabilities of the two atoms, the interaction with the field reduces to

$$H_{int} = -\frac{2\pi I}{c} \left[(\alpha_1 + \alpha_2) + \frac{2\alpha_1\alpha_2}{R^3} (3 \cos^2 \theta - 1) \right]. \quad (2)$$

Introducing a dimensionless reduced length x , $R = \sigma x$, reduced energy e , $E - E_0 = \epsilon e$ (defined with respect to the field shifted dissociation limit $E_0 = -\frac{2\pi}{c}(\alpha_1 + \alpha_2)I$), and reduced laser field intensity i , $I = \beta i$, and replacing all R -dependent terms by their leading order contributions, an asymptotic Schrödinger equation is obtained,

$$\left[-\frac{d^2}{dx^2} - \frac{1}{x^6} + \frac{\mathbf{L}^2}{x^2} - i \frac{\cos^2 \theta - 1/3}{x^3} - e \right] f(x, \theta) = 0. \quad (3)$$

The unit conversion factors are given by

$$\sigma = \left(\frac{2\mu C_6}{\hbar^2} \right)^{1/4}, \quad \epsilon = \frac{\hbar^2}{2\mu\sigma^2}, \quad \beta = \frac{c\sigma^3\epsilon}{12\pi\alpha_1\alpha_2}, \quad (4)$$

and the conversion factor for time is obtained from that of energy, $\tau = \hbar/\epsilon$. For each partial wave ℓ , the wave function is expanded in terms of Legendre polynomials $P_{\ell}(\cos \theta)$

$$f_{\ell}(x, \theta) = y_{\ell}(x) P_{\ell}(\cos \theta), \quad (5)$$

and Eq. (3) is solved in the asymptotic x -domain, imposing to the radial function physical boundary condition at long range and to have a node at $x_{0\ell} > x_{asym} = R_{asym}/\sigma > x_d = R_d/\sigma$, a position separating inner zone and asymptotic outer region, see Ref. [14] for details. The effects of potential $V_g(R)$, centrifugal energy and polarizability in the inner zone can satisfactorily be accounted for by introducing energy-, angular-momentum- and intensity-dependent nodal lines $x_{0\ell}$ [13, 14],

$$x_{0\ell} = x_{00} + A e + B\ell(\ell + 1) + Ci. \quad (6)$$

When the constants A , B and C can be deduced from exact calculations using the Hamiltonian (1) or from experiment, the nodal line technique applied to the asymptotic model fully reproduces the results obtained with (1), cf. Fig. 2 of Ref. [14]. When this is not possible, analytical values for A^G , B^G [13] and C^G [14] which depend on x_{00} , i.e., on the s -wave scattering length, allow for an approximate, universal description of shape resonances, very similar to the asymptotic model developed by Gao for field-free resonances [19].

III. HEURISTIC SCALING RULE

We present and discuss in this section results obtained by solving the Schrödinger equation with the exact

	σ [a ₀]	ϵ [μ K]	β [GW/cm ²]	τ [ns]
⁸⁸ Sr ₂ I	151.053	86.3653	0.635782	88.4409
⁸⁶ Sr ⁸⁸ Sr II	150.617	87.876	0.641319	86.9204
¹³³ Cs ₂	201.843	31.99	0.12048	238.7
⁸⁷ Rb ₂	165.250	72.99	0.25844	104.5

TABLE I: Scaling factors, Eq. (4), for ⁸⁸Sr₂ (case I) and ⁸⁶Sr⁸⁸Sr (case II), obtained for $C_6 = 3246.97 \text{ a}_0^6$ and $\alpha_0 = 186.25 \text{ a}_0^3$, and for ¹³³Cs₂ ($C_6 = 6851.0 \text{ a}_0^6$, $\alpha_0 = 402.20 \text{ a}_0^3$) and ⁸⁷Rb₂ ($C_6 = 4707.0 \text{ a}_0^6$, $\alpha_0 = 309.98 \text{ a}_0^3$).

Hamiltonian (1). Specifically, we consider the shape resonances with field-free $\ell = 4, 8, 12, 16$ for ⁸⁸Sr₂ [16], $\ell = 5, 9$ for ¹³³Cs₂, and $\ell = 2$ for ⁸⁷Rb₂. In paper I [14], a linear dependence of the resonance position vs field intensity was found for the two considered isotopes ⁸⁸Sr₂ and ⁸⁶Sr⁸⁸Sr up to very large values of the intensity [14]. The use of reduced units (see Table I) allows us to extract from these results a general trend for the intensity dependence of the resonance position, valid also for different ℓ values and different species.

To this end, we introduce ‘ ℓ -reduced’ energy shifts or slopes. These are the energy shifts or slopes, in reduced units, divided by $\ell(\ell + 1)$. More precisely, for a field-dressed shape resonance adiabatically correlated to a field-free resonance in the partial wave ℓ , which occurs at the reduced energy $e_r^\ell(i)$ for a non-resonant field of reduced intensity i , the ℓ -reduced energy shift is equal to $\delta e / [\ell(\ell + 1)]$, where $\delta e = e_r^\ell(i) - e_r^\ell(0)$ denotes the shift of the resonance from its field-free position (here, as everywhere else in the paper, the position of a shape resonance is taken with respect to the field shifted dissociation limit). Analogously, we call the quantity $\delta e / [i \ell(\ell + 1)]$ ‘ ℓ -reduced’ slope. The intensity dependence of the ℓ -reduced energy shifts is reported in Fig. 1 for the resonances in strontium, rubidium and cesium mentioned above. Except for the $\ell = 2$ resonance in ⁸⁷Rb₂, an almost linear behavior is observed up to high intensity. Moreover, in the limit of vanishing field all slopes are nearly equal.

Before presenting a calculation of the slopes to first order in the perturbation in Sec. IV, we give here a simple qualitative argument, based on perturbation theory, to justify the approximate proportionality $\propto \ell(\ell + 1)$ of the slope of the resonance position’s intensity-dependence at vanishing intensity. The interaction with the field, given in reduced units by

$$h_{int} = -i/x^3 (\cos^2 \theta - 1/3), \quad (7)$$

can be treated as a perturbation and therefore, to first order, in a single-channel approach. One has thus to calculate the matrix element of h_f with the (single-channel) field-free wave functions $f_\ell^{i=0}(x, \theta)$ (see Eq. (A7) in A)

$$\langle f_\ell^{i=0}(x, \theta) | h_{int} | f_\ell^{i=0}(x, \theta) \rangle = -i \alpha(\ell) \int_{x_{0\ell}}^{\infty} [y_\ell^{i=0}]^2 x^{-3} dx \quad (8)$$

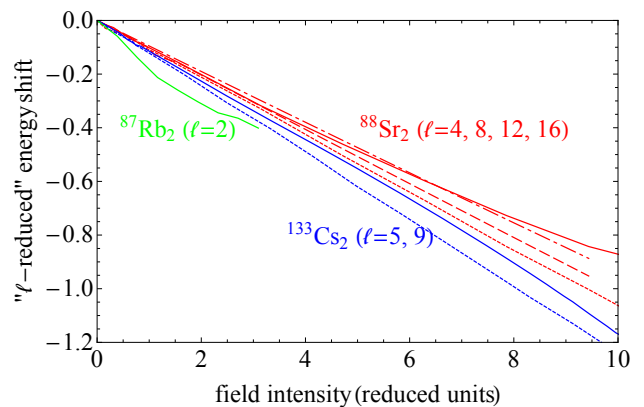


FIG. 1: Intensity dependence of the ‘ ℓ -reduced’ energy shift $\delta e / [\ell(\ell + 1)]$, $\delta e = e_r^\ell(i) - e_r^\ell(0)$, i.e., the shift of the resonance position from its field free value, divided by $\ell(\ell + 1)$. Shown are results obtained with the exact Hamiltonian (1), converted to reduced units, for ⁸⁸Sr₂ (red, $\ell = 4$: full line; $\ell = 8$: dotted line; $\ell = 12$: dashed line; $\ell = 16$: dot-dashed line), ¹³³Cs₂ (blue, $\ell = 5$: full line; $\ell = 9$: dotted line) and ⁸⁷Rb₂ (green, $\ell = 2$: full line).

with $m = 0$ and

$$\alpha(\ell) = \frac{2\ell(\ell + 1)}{3(2\ell + 3)(2\ell - 1)}.$$

A similar integral as the one in Eq. (8) occurs in the expectation value of R^{-3} for field-free wave functions obtained with the exact Hamiltonian (1), when $x_{0\ell}$ is replaced by $R = 0$. It is important to note that the angular factor $\alpha(\ell)$ is nearly independent of ℓ and equal to $\sim 1/6$. The ℓ -dependence of the matrix element, Eq. (8), thus necessary arises from the radial part, i.e., the expectation value of x^{-3} for the field free wave functions.

The field-free resonance positions result from the competition between the van der Waals and centrifugal interactions at intermediate distance, where the amplitude of the resonance wave function is very large. This x -domain is located already in the asymptotic zone, but well before the location x_ℓ of the potential barrier, i.e., $x_{asym} < x_{0\ell} < x \ll x_\ell$. Here $x_{asym} = R_{asym}/\sigma$ and $x_\ell, x_\ell = [\ell(\ell + 1)]^{-1/4}$, is the point where the centrifugal and van der Waals interactions exactly balance each other out. The amplitude of the s -wave ($\ell = 0$) radial wave function, $y_{\ell=0}^{i=0}(x)$, is never resonant and thus always rather small in this x -range. Close to threshold, the van der Waals interaction prevails. Treating the rotational kinetic energy as a perturbation and accounting for the first order introduces a resonant correction proportional to $\ell(\ell + 1)$ in the ℓ -wave radial wave function of the field-free molecule. At intermediate distance $y_{\ell>0}^{i=0}(x) \approx y_{\ell=0}^{i=0}(x) + \ell(\ell + 1)z(x)$. When evaluating the integral in Eq. (8), the zeroth order contribution is small, and in the first order, only the cross term $y_{\ell=0}^{i=0}(x) x^{-3} z(x)$ contributes significantly. As the energy varies, resonant behavior might appear, with a maximum of the radial integral and therefore an energy

	$\ell = 4$	$\ell = 8$	$\ell = 12$	$\ell = 16$
position (red. units)	33.26	139.3	247.2	253.5
position (mK)	2.872	12.03	21.35	21.89
width (red. units)	11.48	0.9159	$2.141 \cdot 10^{-3}$	$8.778 \cdot 10^{-12}$
width (μ K)	991.3	79.11	0.01849	$7.582 \cdot 10^{-10}$

TABLE II: Position and width of the $^{88}\text{Sr}_2$ field-free shape resonances with $\ell=4, 8, 12$ and 16 , both in reduced and physical units, as calculated in paper I [14] in a multi-channel asymptotic model with the nodal line technique.

shift with respect to the field-shifted dissociation limit approximately proportional to $i\alpha(\ell)\ell(\ell+1)$, i.e. proportional to $i\ell(\ell+1)$.

For non-zero non-resonant light, this result remains valid only as long as the interaction with the light can be considered as a perturbation compared to the centrifugal interaction, i.e., for $i \ll 6\ell(\ell+1)x_{0\ell}$, in the x -domain mainly contributing to the integral, i.e., for $x_{0\ell} < x < x_\ell$. Therefore, for a given intensity i , the deviation of the reduced energy shift from the approximate law is larger for smaller ℓ -values.

The observation of an approximately universal intensity-dependence of the reduced energy shifts can be equivalently formulated as follows: In order to shift the position of two shape resonances with field-free rotational quantum numbers ℓ_1 and ℓ_2 in two molecules, 1 and 2, by the same amount, the reduced laser intensities i_1 and i_2 must be related as

$$i_1\ell_1(\ell_1+1) \approx i_2\ell_2(\ell_2+1). \quad (9)$$

We emphasize that this rule provides only the approximate *slope* of the energy variation at $i \rightarrow 0$. To obtain the energy variation itself, one also has to know the field-free reduced energy of the shape resonance, i.e., the s -wave scattering length [13, 20].

IV. SLOPES AT VANISHING INTENSITY FROM PERTURBATION THEORY

Since the intensity dependence of the shape resonance positions appears to be linear up to large values of the field intensity, it is interesting to study the behavior at very low intensity and calculate the slopes at $i = 0$. This procedure requires only free-field calculations, that is a single-channel model. In principle, the perturbation theory has here to be applied to a continuous spectrum. We discuss the example of the $^{88}\text{Sr}_2$ shape resonances with field-free $\ell = 4, 8, 12, 16$, whose positions and widths are recalled in table II. We present results obtained by the single-channel nodal line technique, with a detailed description of the resonance profiles, and compare them to those obtained by solving the Schrödinger equation with Hamiltonian (1), using a discretization of the scattering continuum.

A. Single-channel nodal line technique

The description of the perturbation of a shape resonance by a weak interaction takes a rather simple form in the nodal line formalism. It is described in Appendix A, with no particular shape of the potentials involved in the zero and first order expressions. In the case of interest here, the unperturbed asymptotic Schrödinger equation for the radial wave function of wave ℓ reads, in reduced units,

$$\left[-\frac{d^2}{dx^2} - \frac{1}{x^6} + \frac{\ell(\ell+1)}{x^2} - e \right] y^{(0)}(x) = 0, \quad (10)$$

where we have omitted, compared to Eq. (5), the index ℓ of the radial function $y(x)$ for simplicity. The superscript denotes the order of perturbation theory. The perturbation is given by

$$H_1 = i v(x) = -i \frac{\alpha(\ell)}{x^3}. \quad (11)$$

Let us recall that in the nodal line formalism (see Sec. III B of paper I [14]), Eq.(10) is only solved in the asymptotic x domain, $x > x_0$ (here also the index ℓ is omitted for simplicity). The interactions in the inner zone (potential, rotational kinetic energy) in the zeroth order Hamiltonian are accounted for by the choice of the node position, Eq. (6). In the perturbative treatment, contributions coming from the inner zone due to interaction with the non-resonant field, are present in the first order of perturbation theory and have to be accounted for separately.

In a first step, we ignore the variation of the node position to treat the problem in the outer zone. The reduced slopes of position and width of the resonance can be obtained by calculating the perturbation of the energy profile of the phaseshift characterizing the resonance structure (see Appendix A 2 of paper I [14]). This perturbation, written in the Born approximation [21], cf. Eq. (A8), is equal to $\frac{d}{di}\Delta\delta_{out}(e) = -\pi\mathcal{I}_{out}(e)$ with

$$\mathcal{I}_{out}(e) = -\frac{1}{\pi} \frac{d}{di} \Delta\delta_{out}(e) = -\alpha(\ell) \int_{x_0}^{\infty} \frac{1}{x^3} [y^{(0)}(x)]^2 dx \quad (12)$$

where $F_0(x) = y^{(0)}(x)$ is the field-free energy-normalized physical regular radial function ($F_0(x_0) = 0$). Assuming a Lorentzian shape of the derivative of the phaseshift with respect to energy, one obtains for this derivative in Eq. (12) the right-hand side of Eq. (A6). A simple fit procedure thus yields the slopes at $i = 0$ of both position and width of the resonance at $i = 0$ (cf. first line of Table III and Table IV), except for the extremely narrow resonance with $\ell = 16$, for which the slopes cannot be obtained. The simplified formula of Eq. (A9) gives roughly the same result for the slope of the position as the fitting procedure (compare first and third lines of Table III), except for the narrowest resonance ($\ell = 4$).

The nodal line formalism allows us to also account for the modifications due to the internal part of the perturbation which change the node position x_0 . One can calculate the displacement of the node positions with the complete Hamiltonian (see paper I [14]): For instance, the slopes $\frac{dx_0}{di}$ of the intensity dependence of the node positions at $i = 0$ are listed in the last line of Table III for $\ell = 4, 8, 12, 16$ in $^{88}\text{Sr}_2$. If no reliable data are available for the full potential, it is possible to use a 'universal' value for these slopes (see Eq. (13) in paper I [14]). We show in the appendix that a simple relationship, Eq. (A12), exists between the intensity dependence of the node position and the corresponding modification of the slope of the intensity dependence of the phase shift $\frac{d}{di}\Delta\delta_{in}(e) = -\pi\mathcal{I}_{in}(e)$, corresponding to the contribution of the inner zone, with

$$\mathcal{I}_{in}(e) = -\frac{1}{\pi} \frac{d}{di} \Delta\delta_{in}(e) = +\frac{dx_0}{di} \frac{1}{\pi^2 G_0(x_0)^2}. \quad (13)$$

voir signes Here $G_0(x_0)$ is the value at x_0 of the energy-normalized irregular solution of the Schrödinger equation, which is orthogonal to the physical regular one, $F_0(x) = y^{(0)}(x)$, with a node at x_0 . Adding this quantity to the one coming from Eq. (12) and repeating the above fitting procedure for the sum yields the total slopes of both position and width of the resonance (see the second line in Table III and Table IV). The agreement with the slopes calculated with the full potential is excellent (compare lines 2, 4 and 5 of Table III, and lines 1 and 3 of Table IV).

B. Full potential calculations and discretized continuum

The continuum spectrum obtained when representing the exact Hamiltonian (1) in a box of size R_{max} is discretized and represented by means of L^2 -normalized wave functions with energies $E_n > 0$. Resonances in this discretized spectrum are identified by fitting the rotational constant $\langle 1/(2\mu R^2) \rangle$ as a function of energy to a Lorentzian [13], where the expectation value is computed using energy-normalized wave functions [22, 23]. Very narrow resonances, such as those with $\ell = 8, 12$ or 16 in $^{88}\text{Sr}_2$ (cf. Table II for their widths), appear as δ -functions at the corresponding resonance energy, independent of the size of the box R_{max} . The intensity-dependence of the resonance positions has been fitted to a line in the weak field regime, $I \leq 9 \cdot 10^6 \text{ W/cm}^2$ (~ 0.014 in reduced units). The corresponding slopes are presented in Table V (lines 1 and 2), showing indeed only a weak dependence on the size of the discretization box.

Analogously to the previous subsection, we treat the interaction with the non-resonant light, i.e., the last term in the full Hamiltonian (1), as a perturbation to the field-free Hamiltonian, motivated by the approximately linear dependence of the resonance positions on field intensity

	$\ell = 4$	$\ell = 8$	$\ell = 12$	$\ell = 16$
outer	-0.0791	-0.0710	-0.0602	-
outer+inner	-0.0931	-0.101	-0.100	-
outer*	-0.114	-0.0713	-0.0602	-0.0521
outer+inner*	-0.137	-0.101	-0.100	-0.102
calc cf I	-0.0941	-0.101	-0.100	-0.0954
dx_0/di	$4.417 \cdot 10^{-5}$	$4.525 \cdot 10^{-5}$	$4.873 \cdot 10^{-5}$	$5.497 \cdot 10^{-5}$

TABLE III: Reduced slopes (i.e., slopes in reduced units, divided by $\ell(\ell + 1)$) of the resonance position's intensity dependence for $^{88}\text{Sr}_2$ and $\ell=4, 8, 12$ and 16 from different approaches. The first four lines are obtained with the single-channel perturbative approach described in the Appendix: Lines 1 and 3: including only the asymptotic outer part of the perturbation, Eq. (12). Lines 2 and 4: taking also the inner part through the intensity-dependence of the node position, Eq. (12), into account. The first two lines correspond to a fitting procedure to formula Eq. (A6) of the derivative of the phase shift with respect to e and i . The following two lines (marked by a star) correspond to the simplified formula Eq. (A9), ignoring the slope of the intensity dependence of the width. The fifth line results from a calculation similar to those performed in paper I [14], i.e., with an asymptotic single-channel model with i -dependent nodal lines. The last line lists the slopes of the node position's intensity-dependence used in paper I [14] and required in lines 2 and 4.

	$\ell = 4$	$\ell = 8$	$\ell = 12$	$\ell = 16$
outer	-1.44	-0.213	-0.0000891	-
outer+inner	-1.88	-0.324	-0.000156	-
calc cf I	-1.69	-0.329	-0.000160	-

TABLE IV: Same as Table III but for the width instead of the position of the resonances (lines 2 and 4 are omitted since the simplified formula Eq. (A9) does not give any information on the intensity dependence of the width).

up to fairly large intensity. Time-independent perturbation theory provides the following first-order correction to the field-free energy of the resonances [24, 25],

$$\Delta E_{n,\ell} = -\frac{2\pi I}{c} \left[\langle \psi_{n,\ell} | \alpha_{\perp}(R) | \psi_{n,\ell} \rangle + \langle \psi_{n,\ell} | \Delta\alpha(R) | \psi_{n,\ell} \rangle \frac{2\ell^2 + 2\ell - 1}{(2\ell + 3)(2\ell - 1)} \right], \quad (14)$$

where $\psi_{n,\ell}$ is the field-free L^2 -normalized wave function of the resonance. This correction includes the shift of the field-dressed dissociation limit, $E_0 = -4\pi\alpha/c$. When using additionally the approximation (2) for the interaction Hamiltonian at sufficiently large distance, the first-order correction to the energy shift with respect to E_0 , in reduced units, becomes

$$\Delta e_{n\ell} = -i \langle \psi_{n,\ell} | x^{-3} | \psi_{n,\ell} \rangle \alpha(\ell), \quad (15)$$

equivalent to Eq. (8). Equations (14) and (15) provide an approximation to the slopes of the intensity depen-

	R_{max} [a_0]	$\ell = 4$	$\ell = 8$	$\ell = 12$	$\ell = 16$
exact	$1 \cdot 10^5$	-0.1026	-0.0756	-0.1013	-0.0952
exact	$2 \cdot 10^5$	-0.1010	-0.0754	-0.1017	-0.0952
PT $\langle x^{-3} \rangle$	$1 \cdot 10^5$	-0.137	-0.0681	-0.0900	-0.0827
PT $\langle x^{-3} \rangle$	$2 \cdot 10^5$	-0.133	-0.0692	-0.0904	-0.0827
full PT	$1 \cdot 10^5$	-0.144	-0.0743	-0.1011	-0.0952
full PT	$2 \cdot 10^5$	-0.140	-0.0756	-0.1017	-0.0952

TABLE V: Reduced slopes (i.e., slopes in reduced units, divided by $\ell(\ell + 1)$) of the resonance position's intensity dependence for $^{88}\text{Sr}_2$, computed from fitting a line to the results obtained with the exact Hamiltonian (lines 1 and 2) and computed within perturbation theory, Eq. (15) (lines 3, 4) and Eq. (14) (lines 5, 6) for two different sizes R_{max} of the discretization box. These slopes are to be compared to those reported in Table III.

dence of the resonance positions, valid within the limits of a weak perturbation. These slopes were computed for two different sizes of the discretization box, using the field-free L^2 -normalized wave functions, see Table V. For $\ell = 12$ and 16, the slopes obtained with perturbation theory using the full interaction (14) (lines 5 and 6) are very close to the fit of the field-dressed energy versus i (lines 1 and 2), whereas the slopes obtained when neglecting the R -dependence of the polarizability anisotropy at short range (lines 3 and 4) show some deviation. This indicates the short-range part of the interaction with the non-resonant field to be not completely negligible. Comparing lines 1 and 2 in Table V to Table III allows to assess the accuracy of the single-channel nodal line technique: For $\ell = 12$ and 16, the error is below 10 per cent when using intensity-dependent nodal lines (cf. lines 2 and 4 in Table III). For $\ell = 4$, the agreement between the full calculations and the single channel results is slightly worse. This is not surprising since the intensity dependence of this resonance is not perfectly linear even at low intensity, cf. Fig. 3 of Ref. [16]. Thus this resonance cannot be fully described by perturbation theory. This is evident both from comparing lines 3, 4 and 5, 6 to lines 1, 2 in Table V and also from comparing Table V and Table III.

Finally, for $\ell = 8$, the reduced slopes from the exact calculations are surprisingly close to the less accurate single channel picture, accounting only for the outer, but not the inner region. In fact, the observed agreement of the slopes is accidental, and perturbation theory breaks down in the case of $\ell = 8$. This is due to an avoided crossing occurs with an $\ell = 6$ resonance from an adjacent series which is over the barrier at zero intensity, as illustrated in Figure 2. The avoided crossing causes a discontinuity around 3.5 reduced units in the otherwise linear intensity dependence of the $\ell = 8$ resonance. Since the resonance that comes close to $\ell = 8$ differs from ℓ by only 2, the wavefunctions are coupled considerably even at very low non-resonant field intensity. Consequently, right at the crossing, strong hybridization is observed, with pop-

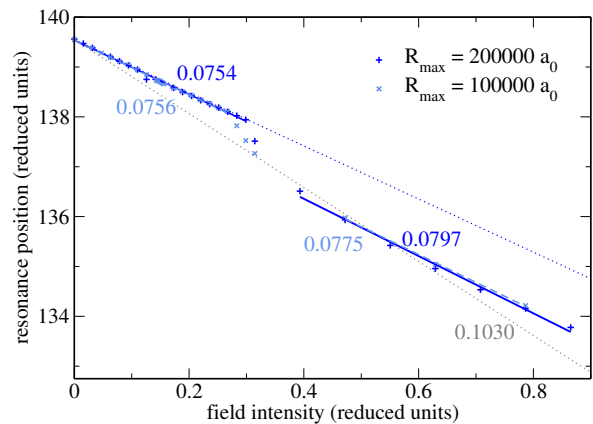


FIG. 2: Intensity dependence of the position of the resonance with $\ell = 8$ in $^{88}\text{Sr}_2$, obtained from calculations with the full potential for two different grid sizes (crosses). The lines represent linear fits to the data, with the numbers annotating the reduced slopes, i.e., the slopes divided by $\ell(\ell + 1)$. The discontinuity is caused by an avoided crossing of the $\ell = 8$ resonance and an over-the-barrier resonance with $\ell = 6$ from the adjacent series. The grey dotted line is obtained when fitting the data over a large interval, ignoring the discontinuity due to the avoided crossing.

ulation distributed almost equally (44% vs 56%) in the $\ell = 6$ and $\ell = 8$ channels. But for intensities just slightly away from the avoided crossing, the mixing goes down to 10% vs. 90%. This explains the perfectly linear intensity dependence that is resumed after the avoided crossing is passed. When fitting the intensity dependence of the resonance position for a range of intensities which includes an avoided crossing, the slope is overestimated. This is indicated by the grey dotted line in Figure 2. Note that the behavior observed for the $\ell = 8$ resonance is truly accidental, since it requires a resonance with $\ell \pm 2$ from an adjacent series to come close by at very weak field. Since this does not happen very often, perturbation theory and the single channel approximation generally work very well, as observed for $\ell = 12$ and 16.

V. SYSTEMATIC SINGLE-CHANNEL CALCULATIONS: GENERAL TRENDS

The good agreement between the perturbation theory results with exact calculations shown in the previous section indicates that a single-channel approximation may be sufficient for many purposes. Specifically, we use the single-channel approximation in section V A to predict the position and width of shape resonances (with no non-resonant field). This extends the approach of Ref. [13], simplifying the required calculations. Second, we employ the single-channel approximation to investigate universality of the intensity-dependence of shape resonances exposed to non-resonant light in section V B.

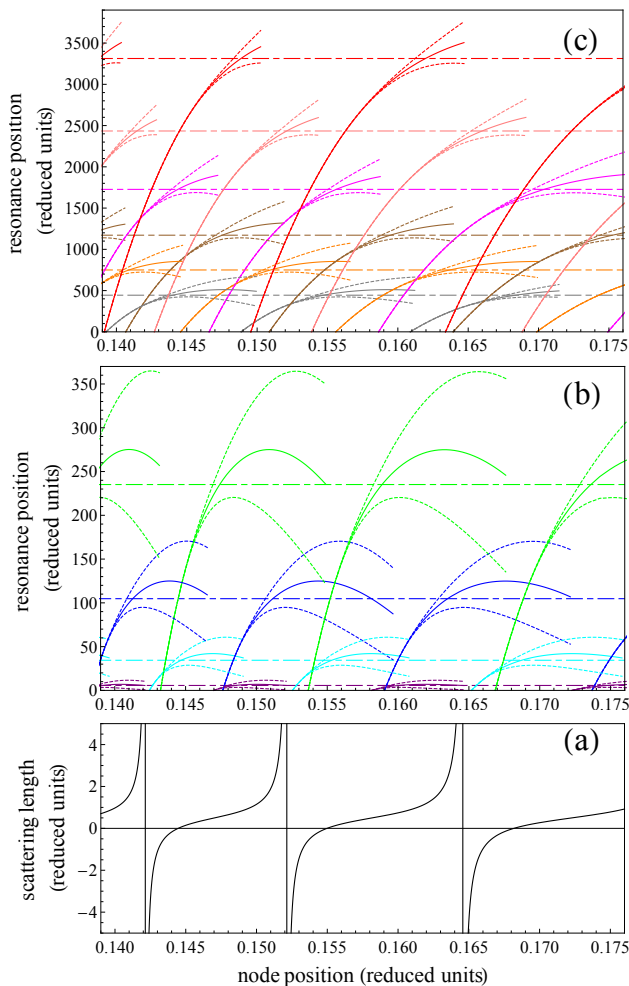


FIG. 3: b,c: Energies (taken with respect to the threshold) and widths of even ℓ -wave shape resonances as a function of the node position $x_{0\ell}$ in a single-channel asymptotic model with energy- and angular momentum-independent nodal lines. The energies, e_r^ℓ , are represented by continuous lines; and the curves $e_r^\ell \pm \gamma^\ell/2$, where γ^ℓ denotes the resonance width, are drawn as dashed lines. The top of the potential barriers, $v_{top}^\ell = 2[\ell(\ell+1)/3]^{3/2}$, are indicated by the horizontal dot-dashed lines (c: $10 \leq \ell \leq 20$, i.e., grey: $\ell = 10$; orange: $\ell = 12$; dark brown: $\ell = 14$; light purple: $\ell = 16$; rose: $\ell = 18$; red: $\ell = 20$. b: $2 \leq \ell \leq 8$: purple: $\ell = 2$; light blue: $\ell = 4$; dark blue: $\ell = 6$; green: $\ell = 8$.) a: s -wave scattering length, in reduced units.

A. Field-free case

In the single-channel asymptotic model using the nodal line technique, the only parameter relevant for the partial wave ℓ is the node position, $x_{0\ell}$, which determines the position and width of shape resonances. The characteristics of the resonances can be determined using the complex energy method, described Sec. A 3 of paper I [14], for narrow resonances or employing the profile of the phase shift, see Sec. A 2 in paper I [14], for

broad resonances close to the top of the potential barrier. The resonance position as a function of node position is shown in Fig. 3 for even ℓ ranging from 2 to 20 and for node positions $0.139 \leq x_{0\ell} \leq 0.176$. In Fig. 3, a single abscissa is used for the various $x_{0\ell}$, which is as if the dependence of the nodal lines energy and angular momentum had been neglected, i.e., it is equivalent to $x_{00} = x_{0\ell}$, or $A = B = 0$ in Eq. (6). The resonance position shows a pseudo-periodic dependence on node position: For each ℓ value, separate branches appear successively, with discontinuities occurring at ℓ -dependent values $x_{0\ell}$ such that $J_{(2\ell+1)/4}(1/(2x_{0\ell}^2)) = 0$, where J_ν denotes a regular Bessel function. When this condition is fulfilled, a bound level with angular momentum ℓ reaches the threshold and becomes a shape resonance. Correspondingly, the number of bound ℓ -levels is decreased by one, as is the number of nodes of the resonance wave function inside the potential barrier, $x_{0\ell} < x < x_\ell$. Between two consecutive discontinuities, along a given branch, the resonance energy increases from threshold, reaches the top of the potential barrier, $v_{top}^\ell = 2[\ell(\ell+1)/3]^{3/2}$, and even passes over the top of the barrier, with the resonance profile becoming very broad. The dependence of the reduced s -wave scattering length on x_{00} (see Eq. (12) of Ref. [13]) is also shown in Fig. 3. It exhibits an analogous pseudo-periodic pattern, and the presence of an $\ell = 0$ bound level just at threshold corresponds, as is well known, to infinite scattering length. One can see in Fig. 3 that, for a given value of the scattering length, there is never more than one resonance below the top of a particular ℓ -potential barrier; and when a resonance appears in a particular ℓ -channel, resonances also appear in the $\ell \pm 4p$ (p integer) channels.

In order to properly account for the contribution of the potential and centrifugal term at short range, $x < x_{00}$, the nodal lines need to depend on both energy and angular momentum [13]. The results presented in Fig. 3 can easily be extended to energy- and angular momentum-dependent node positions $x_{0\ell}$: The dependence on angular momentum simply introduces ℓ -dependent translations parallel to the horizontal axis. The energy-dependence modifies the shape of the curves shown in Fig. 3 only slightly. The position and width of field-free resonances of any molecule can be estimated from Fig. 3, once the nodal lines $x_{0\ell}$, Eq. (6) have been chosen (we use in this section the 'universal' asymptotic model [13], with $A = A^G = -(x_{00})^7/8$, $B = B^G = (x_{00})^5/4$ and $C = 0$, resulting in nodal lines depending only on x_{00}). The results of the transformation $e_r(x_{0\ell}) \rightarrow e_r(x_{00})$ are presented in Fig. 4, with the abscissa now being actually x_{00} . In addition, for the figure to be more compact, we have divided e_r^ℓ by the height of the corresponding rotational barrier v_{top}^ℓ . Figure 4 is useful to predict, at least roughly, the position of shape resonances of a molecule with s -wave scattering length a_S : The resonances lie on the vertical line located at the abscissa $a(x_{00}) = a_S$ (with a_S in reduced units). The dashed vertical lines in Fig. 4 indicate the examples of $^{88}\text{Sr}_2$ and

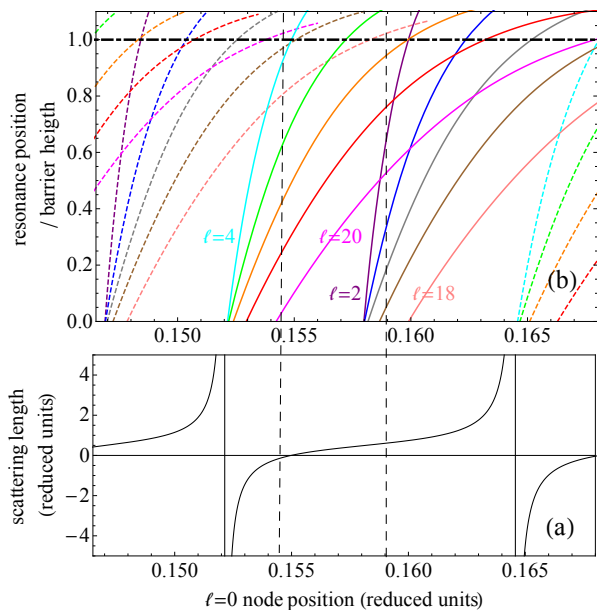


FIG. 4: b: Energy relative to the top of the potential barrier, e_r^ℓ/v_{top}^ℓ , of ℓ -wave shape resonances ($2 \leq \ell \leq 20$ even) as a function of the node position x_{00} (in reduced units) of the s -wave threshold wave function ($e^{\ell=0}(x_{00}) = 0$) in the universal single-channel asymptotic model with energy- and angular momentum-dependent nodal lines ($A = A^G B = B^G$). The relative energies for two $\ell + 4p$ -series (with integer p), $\ell = 2, \dots, 18$ and $\ell = 4, \dots, 20$, are represented by continuous lines; and the three adjacent series by dashed lines (same color code as in Fig. (3)). The horizontal black dot-dashed line indicates the top of the potential barriers. a: s -wave scattering length, $a_S(x_{00})$, as a function of node position. The vertical dashed black lines correspond to $^{88}\text{Sr}_2$ and $^{86}\text{Sr}^{88}\text{Sr}$.

$^{86}\text{Sr}^{88}\text{Sr}$ studied in paper I, with the scattering lengths equal to $a_S = -2a_0$ [26] or -0.013 reduced units and $a_S = 97.9a_0$ [27] or 0.664 reduced units, respectively. Note that, for a given molecule, the resonance energies relative to the barrier tops, e_r^ℓ/v_{top}^ℓ , generally decrease regularly with increasing ℓ . Note also that shape resonances with $\ell = 4p$ (p integer, not too high) appear at threshold for a reduced scattering length with large absolute value, whereas shape resonances with $\ell = 4p + 2$ appear at threshold for a reduced scattering length close to 0.48 . This property had been derived analytically by Gao [28] by solving the Schrödinger equation for a x^{-6} potential plus centrifugal term limited at $x_0^G \rightarrow 0$ by an infinite repulsive wall [28, 29]. With this potential, analytical values for the reduced s -wave scattering length a_ℓ^G and the wall position $x_{0\ell}^G$ for which the last, least-bound rotational levels $\ell = 1, 2, 3, 4$ modulo 4 are located exactly at the dissociation limit, have been obtained [28, 29]. For $x_{00} \rightarrow 0$, the 'universal' asymptotic nodal line model becomes equivalent to Gao's universal model.

For completeness, Fig. 5 presents the widths of the field-free resonances, calculated in the single-channel

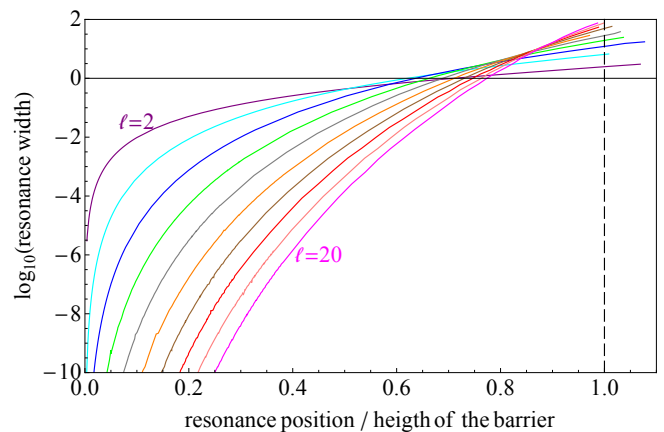


FIG. 5: Resonance widths γ^ℓ as a function of resonance position relative to the centrifugal barrier, e_r^ℓ/v_{top}^ℓ , for ℓ -wave field-free shape resonances (with ℓ even, $2 \leq \ell \leq 20$, same color code as in Fig. 3), obtained by single-channel calculations with energy- and angular momentum-independent nodal lines. The abscissas 0 and 1 correspond to a resonance at threshold and a resonance at the top of the centrifugal barrier, respectively, and the solid black horizontal line indicates the top of the barriers.

asymptotic model, as a function of resonance energy. These widths are already visible in Fig 3, they are represented by the distance between the dotted lines around each resonance. In contrast to Fig 3, Fig. 5 emphasizes the general trend of the widths as a function of energy, relative to the top of the barrier: At threshold, the resonances have a vanishing width, which rapidly increases when the resonance energy increases (note the logarithmic scale). At the top of the potential barrier, the resonance width is rather huge, between 1 to 100 reduced units. This general behavior is observed for all partial waves.

B. Universality in the non-resonant light control of shape resonances at low intensity

The linearity of the intensity dependence of the resonance positions observed in paper I [14] and the validity of perturbation theory at low intensity suggest a more detailed investigation of the field-dressed resonances in the universal asymptotic model. To this aim, we determine the position of the field-dressed resonances, $e_r^\ell(i)$, at very small field intensity ($i = 0.01$ reduced units) as a function of node position $x_{0\ell}$, in the range $0.139 \leq x_{0\ell} \leq 0.176$, and for partial waves with even ℓ -value, with $2 \leq \ell \leq 20$. For the same partial wave and the same $x_{0\ell}$ value, the resonance position without non-resonant field is denoted by $e_r^\ell(0)$. When determining these two resonance positions, the contribution of the non-resonant field is accounted for only in the 'outer' zone, $x > x_{0\ell}$. The contribution of the field to the ℓ -reduced' slope of the resonance position's intensity-dependence in the outer zone can therefore be

quantified as

$$\mathcal{S}_{out} = \frac{e_r^\ell(i) - e_r^\ell(0)}{i l(l+1)}. \quad (16)$$

The contribution of the non-resonant field in the 'inner' zone results, as described in I [14], in a change of the node position proportional to the field intensity. With Eq. (6), this change becomes $dx_{0\ell}/di = C$. The contribution of the field to the ' ℓ -reduced' slope in the inner zone becomes

$$\mathcal{S}_{in} = \frac{1}{l(l+1)} \frac{de_r^\ell(0)}{dx_{0\ell}} \frac{dx_{0\ell}}{di}, \quad (17)$$

where the first derivative is evaluated from the dependence of $e_r^\ell(0)$ on $x_{0\ell}$, reported in Fig. 3. The second derivative is taken to be equal to the value of C , $C = C^G$, in the universal asymptotic model (cf. Eq. (13) in paper I [14]),

$$C^G = -x_{00}^4/12 + 3x_C^4/48. \quad (18)$$

Here, $x_C = R_C/\sigma$ is the position, in reduced units, at which the asymptotic expansion for the polarizabilities is truncated (see Sec. II of paper I [14]). In the universal model, the total reduced slope is equal to $\mathcal{S} = \mathcal{S}_{in} + \mathcal{S}_{out}$ and depends for each ℓ -value on the resonance position, $e_r^\ell(0)$. Calculating $\mathcal{S}(e_r^\ell(0))$ for the same energy $e_r^\ell(0)$ but using different branches for the node $x_{0\ell}$ (see Fig. 3) results in almost the same value. This proves the adequacy of our treatment of the different interactions (potential, rotational energy, laser field interaction) in the inner zone.

Figure 6 presents the total ℓ -reduced slopes \mathcal{S} as a function of the field-free resonance position relative to the height of the potential barrier, $e_r^\ell(0)/v_{top}^\ell$. Although a large number of ℓ values and, in principle, any value of the scattering length is included in the calculations, strikingly, the slopes in Fig. 6 are contained in a rather small interval. The largest deviations occur for the lowest ℓ -values, $\ell = 2$ or 4. For a fixed ℓ -value, the slope increases slightly (i.e., its absolute value decreases) with increasing resonance energy, or, equivalently, with increasing node position $x_{0\ell}$. The absolute value of the ' ℓ -reduced' slope decreases with ℓ . It presents a less pronounced variation when ℓ increases. For ℓ larger than approximately 8, the ' ℓ -reduced' slope is roughly independent of ℓ , with only a weak dependence on the energy relative to the barrier height, $e_r^\ell(0)/v_{top}^\ell$. The mean value of the total ℓ -reduced slopes is $\mathcal{S}(e_r^\ell = 0) = -0.11 \pm 0.2$ at the dissociation limit and $\mathcal{S}(e_r^\ell = v_{top}^\ell) = -0.05 \pm 0.2$ at the top of the potential barrier.

The ℓ -reduced slopes obtained by solving the multi-channel Schrödinger equation with Hamiltonian (1) for the $\ell = 4, 8, 12$ and 16 resonances of $^{88}\text{Sr}_2$, the $\ell = 2$ resonance of $^{87}\text{Rb}_2$ and the $\ell = 5$ and 9 resonances of $^{133}\text{Cs}_2$, reported in Fig. 1, are in very good agreement with the values obtained from the universal asymptotic model, even for the highest ℓ values. The universal model

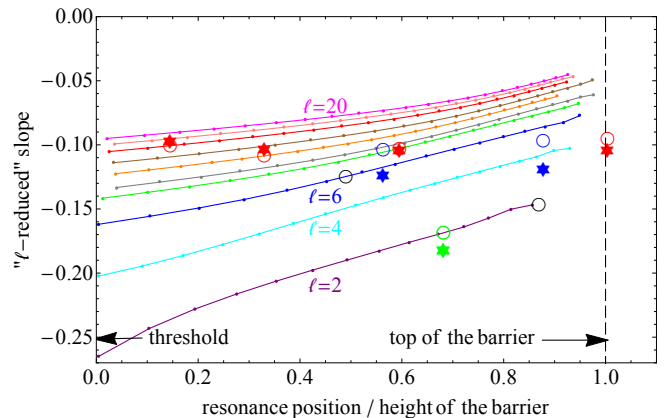


FIG. 6: ' ℓ -reduced' slopes, $\delta e/i/[l(l+1)]$, calculated with a single-channel universal asymptotic model in the limit $i \rightarrow 0$, as a function of $e_r^\ell(0)/v_{top}^\ell$ for even ℓ values $2 \leq \ell \leq 20$ (same color code as in Fig. 3). The contribution of the interaction with the non-resonant light in both outer zone, $x > x_{0\ell}$, and inner zone, $x < x_{0\ell}$, are accounted for, cf. Eqs. (16) and (17). The ' ℓ -reduced' slopes obtained by solving the multi-channel Schrödinger equation for $^{88}\text{Sr}_2$ $\ell = 4, 8, 12, 16$ (red), $^{133}\text{Cs}_2$ $\ell = 5, 9$ (blue) and $^{87}\text{Rb}_2$ $\ell = 2$ (green), cf. Fig. 1, are indicated by stars. The corresponding ' ℓ -reduced' slopes deduced from the universal asymptotic model are indicated by open circles with the same colors as the stars. The values predicted in paper I [14] for the $\ell = 2$ and $\ell = 4$ resonances in $^{86}\text{Sr}^{88}\text{Sr}$, using a multi-channel asymptotic model, are indicated by black open circles.

thus appears suitable to predict, at least approximately, the ℓ -reduced slope for any diatomic molecule. Moreover, we find the heuristic scaling observed in section III to roughly hold in reduced units and for any value of the reduced scattering length. The approximate scaling rule therefore seems to be generally applicable, for a large number of ℓ values and for any dimer.

VI. CONCLUSIONS

We have applied first order perturbation theory to the asymptotic model for shape resonance control of diatomic molecules interacting with non-resonant light developed in Ref. [14]. Our work is the first to employ asymptotic model using the nodal line technique [10] to treat the perturbation of continuum states in the framework of collision theory, i.e., the Born approximation. As in earlier studies applying this approach to shape resonances [13, 14], we find it crucial to properly account for interactions at short range.

The perturbation theory treatment had been motivated by observing a linear dependence of the resonance position on non-resonant field intensity for several molecules with different scattering lengths and shape resonances in different partial waves. Comparison with full multi-channel calculations has revealed our perturbative approach to be valid for not too low values ℓ of the par-

tial waves. The advantage of the perturbative approach is to result in a single-channel model which facilitates calculations significantly. Although the non-resonant field couples partial waves with ℓ and $\ell \pm 2$, we find the single-channel perturbation approximation to be valid up to comparatively high intensity. We rationalize this finding as follows: The first order perturbation correction to the resonance energy is related to the expectation value of x^{-3} (where x denotes the interatomic separation in reduced units). The main contribution to the corresponding radial integral comes from x values just before the centrifugal barrier. In this range, the amplitude of the scattering wave functions is rather small, implying weak coupling, except at energies where a resonance appears. Since, close to threshold, resonances exist simultaneously only for ℓ and $\ell \pm 4$, the resonances themselves are not coupled by the non-resonant field. Therefore an overall only weak channel mixing is observed. The only exception is a resonance with $\ell \pm 2$ from an adjacent series coming close in energy at very low field. In this case, the linear intensity dependence is interrupted by discontinuities, indicating the break-down of perturbation theory at the avoided crossing. However, a single channel approximation is still able to correctly predict the overall slope. That is, one only has to take care to determine the slope from a sufficiently small intensity range where no avoided crossing occurs.

We have analyzed the linear dependence of the resonance position on non-resonant field intensity by introducing reduced slopes, where the shift of the resonance position from its field-free value is divided by $\ell(\ell+1)$. We have observed an almost identical value for the reduced slope of several shape resonances in strontium, rubidium and cesium. The approximately identical dependence of the reduced slope on the energy, relative to the height of the centrifugal barrier, is reproduced by systematic calculations using the universal asymptotic model, where the field-free scattering length is the only free parameter. Our universal model is equivalent to the multi-channel quantum defect treatment of shape resonances developed by Gao [19, 20, 28]. Fixing the value of the field-free scattering length in the universal model allows for predicting the position of field-free shape resonances [13, 20]. The corresponding predictions of our perturbative approach are more accurate for lower partial waves. In contrast, the slopes of the intensity-dependence of the resonances are well predicted even for high ℓ -values.

For all partial waves except for $\ell = 2$, the reduced slopes are found to vary regularly and in a small interval from the dissociation limit, where the resonances emerge, to the top of the centrifugal barrier, where the resonances start to dissolve. This behavior is furthermore independent of the specific molecule, it depends neither on its reduced mass, nor on its C_6 coefficient, polarizability or scattering length, characteristic of the short range interaction. The stability of the reduced slope, derived here by generalizing observations for a small number of molecules and partial waves, presents a universal trend

for field-dressed shape resonances.

The perturbative treatment developed here allows for a simple and efficient approach to determine the intensity-dependence in non-resonant light control of shape resonances since it requires single-channel calculations using the field-free resonance functions only. The slopes predicted by perturbation theory are sufficient to estimate, at least approximately, the non-resonant field intensities that are required to shift a field-free resonance to a desired position. This is important for utilizing non-resonant light control in molecule formation via photoassociation [16] or Feshbach resonances [17]. In addition to tuning the position and width of shape or Feshbach resonances, non-resonant light control can also be employed to change the s -wave scattering length. This will be studied in detail elsewhere [30].

Acknowledgments

Laboratoire Aimé Cotton is "Unité Propre UPR 3321 du CNRS associée à l'Université Paris-Sud", member of the "Fédération Lumière Matière" (LUMAT, FR2764) and of the "Institut Francilien de Recherche sur les Atomes Froids" (IFRAF). R.G.F. gratefully acknowledges a Mildred Dresselhaus award from the excellence cluster "The Hamburg Center for Ultrafast Imaging Structure, Dynamics and Control of Matter at the Atomic Scale" of the Deutsche Forschungsgemeinschaft and financial support by the Spanish Ministry of Science FIS2011-24540 (MICINN), grants P11-FQM-7276 and FQM-4643 (Junta de Andalucía), and by the Andalusian research group FQM-207.

Appendix A: Perturbation of a shape resonance in the nodal line asymptotic model

The description of the perturbation of a shape resonance by a weak interaction takes a rather simple form in the nodal line formalism. For simplicity, the following derivation assumes the use of reduced units, but no particular forms for the radial potentials involved in the zero order H_0 and first order H_1 Hamiltonians.

We consider a shape resonance associated to a Hamiltonian H_0 with position e_{r0} and width γ_0 . Let us assume that the resonance is characterized by a Lorentzian profile of the derivative $\delta'_0(e)$ of the phaseshift with respect to energy, (see for instance Eq. (1.185) in Ref. [21]),

$$\delta'_0(e) = \frac{\gamma_0/2}{(e - e_{r0})^2 + (\gamma_0/2)^2}. \quad (\text{A1})$$

In the nodal line asymptotic formalism, the energy-normalized radial wave function $y^{(0)}$ for any ℓ value at any value of scattering energy $e = k^2$ can be obtained from two separate inward integrations in which the asymptotic behavior of the energy-normalized solution is

imposed to be either $\sin(kx)/\sqrt{\pi k}$ or $\cos(kx)/\sqrt{\pi k}$, with respective solutions $f_0(x)$ and $g_0(x)$ (see Sec. 2 in I). The condition imposed to the physical solution $y^{(0)}$ is to vanish at the node position $x = x_0$. The corresponding phaseshift is given by

$$\tan[\delta_0(e)] = -\frac{g_0(x_0)}{f_0(x_0)}. \quad (\text{A2})$$

The solution $y^{(0)}$ is identical to the regular wave function $F_0(x)$ associated to H_0 , with an asymptotic behavior $\sin(kx + \delta_0(e))/\sqrt{\pi k}$ (see Ref.[13]),

$$F_0(x) = \sin[\delta_0(e)]f_0(x) + \cos[\delta_0(e)]g_0(x). \quad (\text{A3})$$

The linearly independent solution associated to $F_0(x)$ is the irregular wave function $G_0(x)$ given by

$$G_0(x) = +\cos[\delta_0(e)]f_0(x) - \sin[\delta_0(e)]g_0(x). \quad (\text{A4})$$

Let us add a small perturbation characterized by a Hamiltonian $H_1 = i v(x)$, where the parameter i characterizes the strength of the perturbation. We assume the profile of the resonance to remain Lorentzian in the presence of this small perturbation, with the new profile depending on i ,

$$\delta'(e) = \frac{\gamma(i)/2}{(e - e_r(i))^2 + (\gamma(i)/2)^2}. \quad (\text{A5})$$

Close to $i = 0$, the i -dependence of $\delta'(e)$ is related to the derivatives at $i = 0$ of the i -dependencies of position and width:

$$\frac{d}{di}\delta'(e) = \frac{de_r}{di} \frac{\gamma_0(e - e_{r0})}{[(e - e_{r0})^2 + (\gamma_0/2)^2]^2} + \frac{d\gamma}{di} \frac{1}{2} \frac{(e - e_{r0})^2 - (\gamma_0/2)^2}{[(e - e_{r0})^2 + (\gamma_0/2)^2]^2}. \quad (\text{A6})$$

The i -dependence of the phaseshift can be related to the Hamiltonian H_1 : For any e , the additional phase-shift $\Delta\delta_{out}(e)$ coming from the perturbation in the outer asymptotic domain $x > x_0$ is given, to first order in i , by the Born approximation (see for instance Eq. (4.38) in Ref. [21]):

$$\Delta\delta_{out}(e) \sim \tan \Delta\delta_{out}(e) = -i\pi \int_{x_0}^{\infty} v(x)[y^{(0)}(x)]^2 dx \quad (\text{A7})$$

where x_0 is the position of the node, such that

$$\frac{d}{di}\Delta\delta_{out}(e) = -\pi \int_{x_0}^{\infty} v(x)[y^{(0)}(x)]^2 dx = -\pi\mathcal{I}_{out}(e) \quad (\text{A8})$$

The derivative with respect to e of the last equation has to be fitted to Eq. (A6), allowing us to determine the derivatives with respect to intensity at $i = 0$ of position and width of the field-dressed resonance.

For narrow resonances, the i -dependence of the width is weak and the corresponding term in $\frac{d\gamma}{di}$ can be neglected compared to the other one. This implies that the

integral in Eq. (A8) has a Lorentzian shape, with the same center e_{r0} and width γ_0 as $\delta'_0(e)$ (Eq. A1). If we call \mathcal{I}_m the value of the integral $\mathcal{I}_{out}(e)$ at $e = e_{r0}$, we deduce the slope of the i -dependence of the resonance position at $i = 0$ to be

$$\frac{d}{di}e_r = +\pi\mathcal{I}_m\gamma/2 = \int_{-\infty}^{\infty} \mathcal{I}_{out}(e) de, \quad (\text{A9})$$

which is equal to the strength of the interaction integrated over the whole energy-profile. For an attractive potential $v(x) < 0$, the integral $\mathcal{I}(e)$ and therefore the slopes $\frac{de_r}{di}$ are negative and $\Delta_{out}(e)$, Eq. (A7), is positive.

The nodal line formalism also allows to account for the perturbation due to the internal part of the perturbation H_1 at $x < x_0$, which introduces a shift Δx proportional to i in the node position. A simple relationship between Δx and the corresponding modification to first order in i of the phaseshift $\Delta\delta_{in}(e)$ can be obtained from Eq.(A2)

$$\frac{d}{dx_0}\Delta\delta_{in}(e) = -\frac{W(g_0, f_0)}{f_0(x_0)^2 + g_0(x_0)^2}, \quad (\text{A10})$$

where $W(g_0, f_0) = g_0 f'_0 - g'_0 f_0$ denotes the Wronskian (here the derivatives are taken with respect to x). Employing the property $F_0(x_0) = 0$ and the relation between the pairs of functions (f_0, g_0) and (F_0, G_0) ,

$$W(g_0, f_0) = W(G_0, F_0) = \frac{1}{\pi} \quad (\text{A11})$$

$$f_0(x_0)^2 + g_0(x_0)^2 = F_0(x_0)^2 + G_0(x_0)^2 = G_0(x_0)^2,$$

we find

$$\frac{d}{dx_0}\Delta\delta_{in}(e) = -\frac{1}{\pi G_0(x_0)^2}. \quad (\text{A12})$$

Finally, the contribution of the inner zone to the variation of the phaseshift is, for any value of energy,

$$\frac{d}{di}\Delta\delta_{in}(e) = -\frac{dx_0}{di} \frac{1}{\pi G_0(x_0)^2}. \quad (\text{A13})$$

For an attractive potential $v(x)$, the shift in the node position is negative (see the value of C^G in Eq. (13) in paper I [14]) and $\Delta\delta_{in}(e)$ is positive.

This additional correction to the phaseshift coming from the the inner part of the perturbation also results in a shift of the resonance position. This contribution Eq. (A13) is to be added to the slope due to the asymptotic part of the perturbation Eq. (A8). As above the derivative with respect to e of the total slope of the change in the phaseshift associated with the perturbation H_1

$$\frac{d}{di}\Delta\delta(e) = \frac{d}{di}\Delta\delta_{out}(e) + \frac{d}{di}\Delta\delta_{in}(e) = -\pi\mathcal{I}(e). \quad (\text{A14})$$

has to be fitted to Eq.(A6) to determine the slopes at $i = 0$ in the variation of the energy position and width of the field-dressed resonances.

-
- [1] M. J. Seaton and L. Steenman-Clark, *J. Phys. B* **10**, 2639 (1977).
- [2] C. Greene, U. Fano, and G. Strinati, *Phys. Rev. A* **19**, 1485 (1979).
- [3] F. H. Mies, *J. Chem. Phys.* **80**, 2514 (1984).
- [4] F. H. Mies and P. S. Julienne, *J. Chem. Phys.* **80**, 2526 (1984).
- [5] B. Gao, *Phys. Rev. A* **58**, 4222 (1998).
- [6] B. Gao, *Phys. Rev. A* **64**, 010701 (2001).
- [7] K. Jachymski, M. Krych, P. Julienne, and Z. Idziaszek, *Phys. Rev. Lett.* **110**, 213202 (2013).
- [8] K. Jachymski, M. Krych, P. S. Julienne, and Z. Idziaszek, *Phys. Rev. A* **90**, 042705 (2014).
- [9] A. Crubellier and E. Luc-Koenig, *J. Phys. B* **39**, 1417 (2006).
- [10] A. Crubellier, O. Dulieu, F. Masnou-Seeuws, M. Elbs, H. Knöckel, and E. Tiemann, *Eur. Phys. J. D* **6**, 211 (1999).
- [11] B. Pasquiou, G. Bismut, Q. Beaufils, A. Crubellier, E. Maréchal, P. Pedri, L. Vernac, O. Gorceix, and B. Laburthe-Tolra, *Phys. Rev. A* **81**, 042716 (2010).
- [12] N. Vanhaecke, C. Lisdat, B. Tjampens, D. Comparat, A. Crubellier, and P. Pillet, *Eur. Phys. J. D* **28**, 351 (2004).
- [13] B. E. Londoño, J. E. Mahecha, E. Luc-Koenig, and A. Crubellier, *Phys. Rev. A* **82**, 012510 (2010).
- [14] A. Crubellier, R. González-Férez, C. P. Koch, and E. Luc-Koenig, arXiv:1412.0569v1 (2014).
- [15] R. Ağanoglu, M. Lemeshko, B. Friedrich, R. González-Férez, and C. P. Koch, arXiv:1105.0761 (2011).
- [16] R. González-Férez and C. P. Koch, *Phys. Rev. A* **86**, 063420 (2012).
- [17] M. Tomza, R. González-Férez, C. P. Koch, and R. Moszynski, *Phys. Rev. Lett.* **112**, 113201 (2014).
- [18] M. Tomza, W. Skomorowski, M. Musiał, R. González-Férez, C. P. Koch, and R. Moszynski, *Mol. Phys.* **111**, 1781 (2013).
- [19] B. Gao, *J. Phys. B* **36**, 2111 (2003).
- [20] B. Gao, *Phys. Rev. A* **80**, 012702 (2009).
- [21] H. Friedrich, *Theoretical Atomic Physics* (Springer-Verlag Berlin Heidelberg New York, 1998), 2nd ed.
- [22] E. Luc-Koenig, M. Vatasecu, and F. Masnou-Seeuws, *EPJD* **31**, 239 (2004).
- [23] R. González-Férez, M. Weidemüller, and P. Schmelcher, *Phys. Rev. A* **76**, 023402 (2007).
- [24] B. Friedrich and D. Herschbach, *Phys. Rev. Lett.* **74**, 4623 (1995).
- [25] R. González-Férez and P. Schmelcher, *New J. Phys.* **11**, 055013 (2009).
- [26] A. Stein, H. Knöckel, and E. Tiemann, *Eur. Phys. J. D* **57**, 171 (2010).
- [27] J.-C. Zhang, Z.-L. Zhu, Y.-F. Liu, and J.-F. Sun, *Chin. Phys. Lett.* **28**, 123401 (2011).
- [28] G. B., *Eur. Phys. J. D* **31**, 283 (2004).
- [29] J. M. Moritz, C. Eltschkai, and H. Friedrich, *Phys. Rev. A* **63** (2002).
- [30] A. Crubellier, R. González-Férez, C. P. Koch, and E. Luc-Koenig, *Controlling the scattering length with non-resonant light: Predictions of an asymptotic model*, in preparation.